

High Speed ^1H Spectroscopic Imaging in Human Brain by Echo Planar Spatial-Spectral Encoding

Stefan Posse, Gioacchino Tedeschi, Robert Risinger, Robert Ogg, Denis Le Bihan

We introduce a fast and robust spatial-spectral encoding method, which enables acquisition of high resolution short echo time (13 ms) proton spectroscopic images from human brain with acquisition times as short as 64 s when using surface coils. The encoding scheme, which was implemented on a clinical 1.5 Tesla whole body scanner, is a modification of an echo-planar spectroscopic imaging method originally proposed by Mansfield *Magn. Reson. Med.* 1, 370–386 (1984), and utilizes a series of read-out gradients to simultaneously encode spatial and spectral information. Superficial lipid signals are suppressed by a novel double outer volume suppression along the contours of the brain. The spectral resolution and the signal-to-noise per unit time and unit volume from resonances such as *N*-acetyl aspartate, choline, creatine, and inositol are comparable with those obtained with conventional methods. The short encoding time of this technique enhances the flexibility of *in vivo* spectroscopic imaging by reducing motion artifacts and allowing acquisition of multiple data sets with different parameter settings.

Key words: proton spectroscopy; spectroscopic imaging; echo planar encoding; human brain.

INTRODUCTION

Proton spectroscopic imaging (HSI) is increasingly being used to study human brain metabolism (1–11). Brain tumors (1, 6, 8, 10), multiple sclerosis (5, 10), brain infarction (7), epilepsy (2), and acquired immunodeficiency syndrome (4) manifest locally altered metabolite levels. At the same time clinical applications of HSI have been limited by the procedure's length which tests patient tolerance and limits the integration of HSI with diagnostic imaging. Recently, a method based on multiple individually phase encoded spin echoes has been proposed to reduce scan times (12). However, short echo time measurements are not feasible with this technique, because it uses echoes at different echo times. It also has a limited spectral resolution and suffers from T_2 -weighting in k -space. Methods using chemical shift encoded fast scans have similar limitations (13–16).

Echo-planar spectroscopic imaging (EPSI), a much faster method proposed by Mansfield and further devel-

oped by others, avoids these limitations by using a series of periodically inverted gradients to generate a train of echoes that contain both spatial and spectral information (17–23). However, initial implementations suffered from limitations in gradient performance and from spectral artifacts due to the convolution of spectral and spatial information. Recently, we have improved the EPSI-based acquisition technique by enhancing the orthogonalization (separation) of the spectral and spatial information within the hardware constraints of a clinical whole-body scanner and demonstrated short echo time three-dimensional spatial encoding in human brain in clinically feasible acquisition times (24).

Here, we investigate the feasibility of short echo time (13 ms) two-dimensional EPSI in human brain with acquisition times as short as 64 s by using surface coils to improve the signal-to-noise ratio (SNR). The spatial suppression of strong lipid signals in the proximity of the surface coil is improved by a modified pulse sequence which permits localized tuning of the spatial suppression RF pulses. The SNR of *N*-acetyl aspartate (NAA) is evaluated for different acquisition times, voxel sizes, and locations with respect to the surface coil. We also evaluate gradient performance and robustness of the localization scheme.

MATERIALS AND METHODS

For echo-planar spatial-spectral encoding, a trapezoidal read out gradient was inverted periodically to encode k -space in a zig-zag trajectory (Fig. 1). The solid line trajectory corresponds to the original encoding scheme proposed by Mansfield (17) where the length of each trapezoid (τ) corresponds to the inverse of the spectral width in the reconstructed spectra. Reversal of the read-out gradient in the presence of local magnetic field inhomogeneities and asymmetries in gradient switching introduce periodicities in k -space that lead to aliasing artifacts. Aliasing can be removed by separating (editing) the echoes obtained with positive and negative gradients at the expense of reducing the spectral width to $1/(2\tau)$ (17, 19, 20, 22). Evolution in time convolves spectral and spatial information which leads to chemical shift artifacts. To simultaneously eliminate aliasing and to reduce chemical shift artifacts while retaining the desired spectral width ($1/\tau$), we employ spatial-spectral oversampling as represented by the dotted-line trajectories in Fig. 1. For example, when using an oversampling ratio (n) of 2, the read-out gradient strength doubles, thus reducing chemical shift artifacts twofold. After even/odd echo editing (Fig. 2) and time reversal of echoes obtained with negative gradients, the data sets are reconstructed separately and the results are added together to maintain the SNR.

MRM 33:34–40 (1995)

From the Diagnostic Radiology Department, The Warren Grant Magnuson Clinical Center (S.P., D.L.B.), the Neuroimaging Branch, National Institute of Neurological Disorders and Stroke (G.T.) and the Section on Clinical Pharmacology, National Institute of Mental Health (R.R.), National Institutes of Health, Bethesda, Maryland and St Jude Children's Research Hospital, Memphis, Tennessee (R.O.).

Address correspondence to Stefan Posse, Ph.D, Institute of Medicine, Research Center Jülich GmbH, P.O. Box 1913, D-52425 Jülich, Germany. Received July 14, 1994; revised October 11, 1994; accepted October 12, 1994.

1994 SMR Young Investigators' Rabi Award Finalist.

0740-3194/95 \$3.00

Copyright © 1995 by Williams & Wilkins

All rights of reproduction in any form reserved.

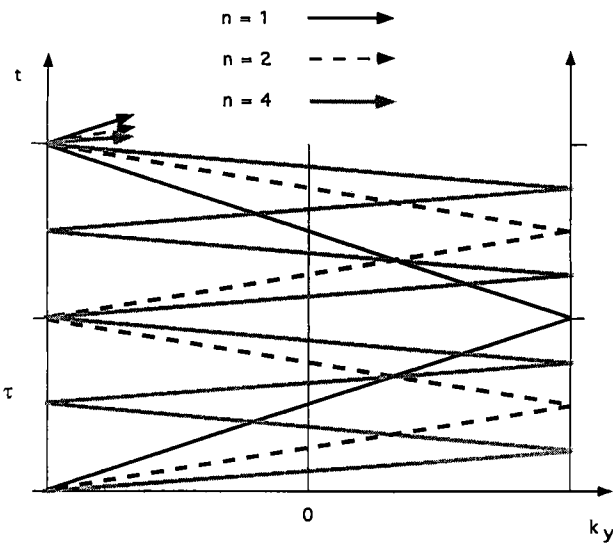


FIG. 1. K_y - t space trajectories of EPSI acquisition methods with different spatial-spectral oversampling ratios (n). The time interval τ determines the desired spectral width $1/\tau$ in the reconstructed spectra. The k_x domain, which is orthogonal to the k_y - t plane, is not shown.

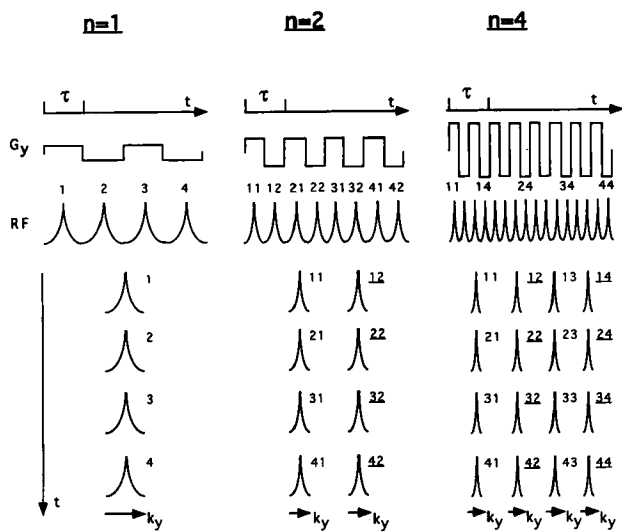


FIG. 2. Echo editing scheme for an individual EPSI data trace obtained with different oversampling ratios (n). With two-fold oversampling ($n = 2$) two echo trains from alternate echoes are obtained. With four-fold oversampling ($n = 4$) four echo trains are obtained. Two-dimensional Fourier transformation of these echo trains provides a series of spatially localized spectra.

The method was implemented on a clinical 1.5 Tesla whole body scanner (GE Medical Systems, Milwaukee, WI) with actively shielded gradients of 10 mT/m strength. Spatial-spectral encoding with twofold oversampling was performed along the y -axis. At 1.5 Tesla a spectral width of 488 Hz covers almost all signals that are observable *in vivo* (between 0 and 7.64 ppm). The length of each read-out gradient lobe was 1024 μ s. For spatial resolutions between 5 and 10 mm, the read-out gradient amplitudes were between 4.6 and 2.3 mT/m, and the gradient ramp times were limited by hardware between

160 and 80 μ s. Due to the convolution of spatial and spectral information, the water signal could be positioned on resonance and any signal outside of a frequency range of ± 244 Hz would alias back into the spectrum. For each data trace 16384 complex data points ($=512$ spectral points $\times 32$ spatial points) were sampled continuously with a spectral width of 32 kHz to yield a digital frequency resolution of 1.9 Hz. No gradient tuning was required. The x -dimension was localized with conventional 32 step phase encoding.

Volume prelocalization of an axial slice was obtained by a three-pulse sequence to generate a stimulated echo (Fig. 3) (24). Surface lipid were suppressed by a series of eight slice selective suppression pulses with gradient dephasing (SS1), each of which suppressed a different slice positioned along the brain contours and orthogonal to the stimulated echo selected axial slice. The position and orientation of each suppression slice could be adjusted individually. The series of suppression pulses was repeated during the TM period (SS2) to improve lipid suppression. For localized tuning of the suppression RF pulses, the slice selective stimulated echo pulse sequence could be converted into a volume selective pulse sequence to receive signal only from a selected suppression slice. This was accomplished by changing the orientation of the slice selection gradient of the last RF pulse (Fig. 3). The residual signal from a selected suppression slice could be observed in spectroscopy mode to minimize residual lipid signals or in imaging mode for spatially resolved tuning.

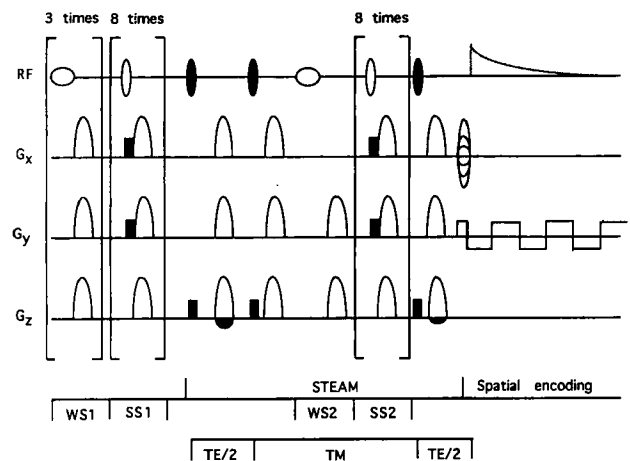


FIG. 3. Water suppressed EPSI pulse sequence with volume prelocalization. An axial slice is selected by three RF pulses (gray symbols) to form a stimulated echo. Spatial suppression (SS1, SS2) is applied orthogonal to the axial slice to suppress superficial lipid signals. Eight spatial suppression pulses with subsequent gradient dephasing are applied during each presaturation period (SS1, SS2) in different spatial orientations and locations along the brain contours. Three CHESS water suppression pulses are applied in front of the prelocalization scheme (WS1) and one CHESS pulse is applied during TM (WS2). Spatial localization is achieved by Echo-Planar spectral-spatial encoding along the y -axis and phase encoding along the x -axis. For localized suppression slice tuning, the orientation of the slice selection gradient of the last RF pulse is changed (see Methods).

Three chemical shift selective water suppression pulses (CHESS) with 50 Hz bandwidth were applied before the localization scheme. The flip angles and timing sequence of the water suppression pulses were numerically optimized (25). A fourth water suppression pulse was applied during the TM period to further enhance water suppression. With this slice selective pulse sequence, the gradient dephasing requirements during the $TE/2$ periods were strongly reduced with respect to volume selective stimulated echo methods. Thus, the motion sensitivity was similar to that of previously published methods (10), despite the longer TM period. Signal losses due to J -modulation and due to zero-quantum modulations during TM were minimized by using short echo times (26).

Protocol

Measurements were performed on five normal volunteers and on some patients with neuropsychiatric disorders. Informed consent was obtained from all subjects prior to the measurements according to institutionally reviewed protocols. In these studies, different anatomical regions, including occipital brain, frontal brain and cerebellum, were investigated using a circular receive-only surface coil (12.7-cm diameter) with body coil excitation. FDA guidelines for RF power deposition were observed and hearing protection was provided. Fast spin echo scans (TE : 85 ms, TR : 2s, 8 echoes) or gradient recalled echo scans (TE : 5 ms, TR : 33 ms, flip angle: 30°) were acquired to locate the volume of interest. In some cases, we used automatic higher order shimming based on phase sensitive gradient echo imaging, as described by Webb and Macowski (27). Water-suppressed and nonwater-suppressed spectroscopic imaging data were acquired at TR : 2000 ms, TE : 13 ms, and TM: 120 ms from 1- or 2-cm thick axial slices. Data acquisition and echo-planar gradient encoding started 1 ms prior to the top of the stimulated echo to minimize first order phase errors in the spectra. The minimum acquisition time for a 32×32 spatial matrix was 64 s. When necessary, averaging was performed to improve the SNR.

Data Processing

Data processing was performed off-line using the SA/GE software (GE Medical Systems, Milwaukee, WI) on a SUN Sparc II workstation. Data representing "even" and "odd" echoes were rearranged as shown in Fig. 2 to yield separate data sets that had conventional data format and that could be processed separately. Spectral filtering consisted of 3 or 4 Hz exponential line-broadening. Fermi filtering in the spatial domains (radius: 16 points, width: 4 points) reduced Gibb's ringing. Residual water signals were removed by low frequency filtering in the time domain: A 131 point binomial filter was applied to the spatially localized time domain data, and the result was subtracted from the original time-domain data. Absorption mode spectra from the two data sets were added after automatic and manual zero order phase correction to maintain signal-to-noise. Magnitude spectroscopic images were created by spectral integration over a spectral width of 12 Hz.

RESULTS

In vitro studies performed on a daily quality assurance phantom (GE Medical Systems, Milwaukee, WI) that contained water and glycerol confirmed that the spatial localization obtained with EPSI in 64 s was similar to that of conventional HSI acquired in 32 min (Fig. 4). A slight loss in spatial resolution due to continuous data sampling during the gradient ramps (10–20% depending on the gradient ramp time) was only apparent before spatial filtering was performed. Spectral resolution and spectral artifacts with either method were similar (Fig. 5), suggesting only minor eddy current effects due to the oscillating read-out gradient. The SNR of EPSI obtained in 1 min *in vitro* was approximately 5–6 times less than that in conventional HSI acquired in 32 min, a result consistent with the shorter acquisition time. We investigated possible localization errors caused by interactions with local susceptibility related gradients by changing shim gradients. We detected no significant spectroscopic image distortions for the range of shim currents typically used *in vivo*, despite significant line broadening in localized spectra. The amplitude of the dephasing gradient lobe could be changed by up to 10% without noticeable changes in localization. Gradient tuning and stability were verified by prelocalizing a $3 \times 3 \times 1$ cc volume in a homogeneous phantom containing distilled water. The volume was shimmed to a line width of 2 Hz. In the k_y - t plane, the symmetry of the magnitude and the phase of a selected echo train demonstrate excellent gradient performance (Fig. 6).

In vivo measurements were acquired in 1–16 min and with voxel sizes ranging from 0.4–2 cc (Figs. 7 and 8).

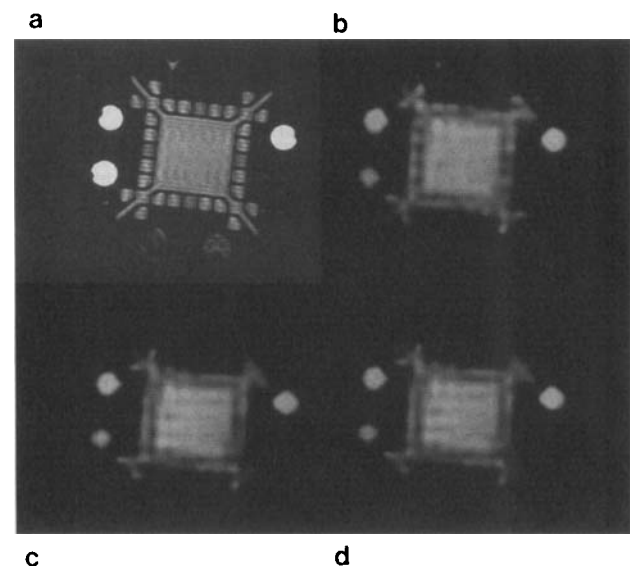


FIG. 4. Comparison between conventional HSI and EPSI on a daily quality assurance phantom obtained with a quadrature head coil. (a) Gradient echo localizer (TE : 5 ms, TR : 100 ms, α : 45° , FOV: 24 cm). (b) Conventional spectroscopic image obtained with phase encoding in 32 min. This image was obtained by integration over the entire spectral range. (c, d) Spectroscopic images obtained with EPSI in 1 min. (c) Integrated image computed from even echo data. (d) Integrated image computed from odd echo data (TE : 13 ms, TR : 1 s, TM: 120 ms, Matrix: 32×32 , Number of averages: 2).

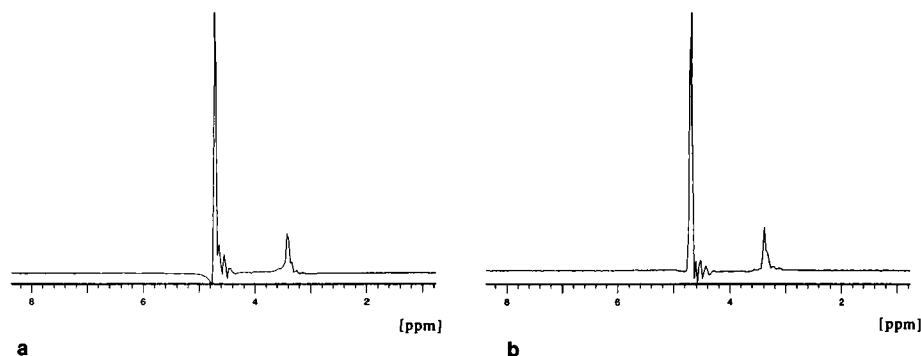


FIG. 5. Selected individual spectra from the data sets in Fig. 4. (a) Conventional HSI. The two resonances represent water (on resonance) and glycerol (off resonance). The EPSI spectrum (b) was obtained by adding absorption mode spectra from the even- and odd-echo data sets in Fig. 4. The total spectral range of 7.64 ppm is shown and demonstrates the absence of aliasing artifacts. There is little evidence for additional eddy current effects due to the EPSI read-out gradients (see distortions to the right of the water line).

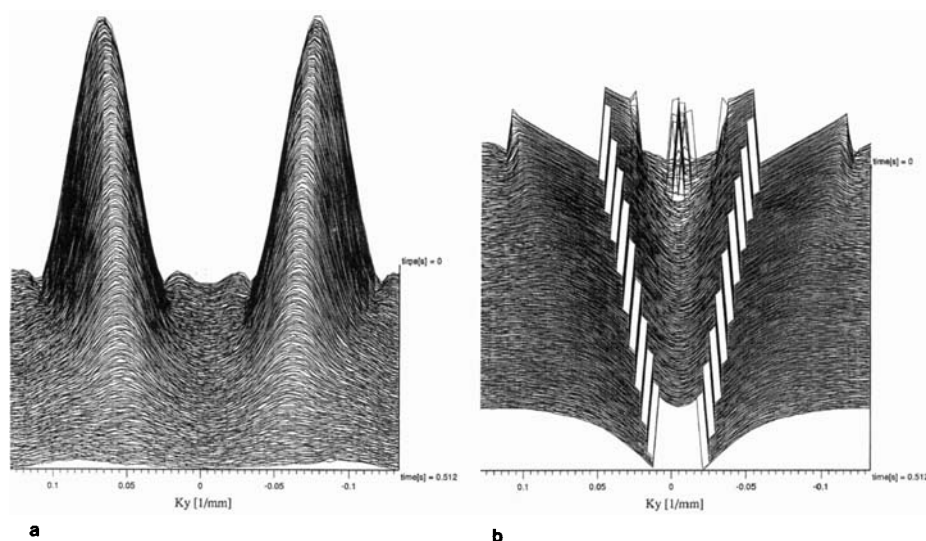


FIG. 6. Single raw data trace from an EPSI data set after echo editing. The two echo trains correspond to the even-odd echo data format shown in Fig. 2. (a) Echo magnitudes. (b) Echo phases (prelocalized volume: $3 \times 3 \times 1$ cc, spatial resolution: 7.5 mm).

The spectral pattern was similar to that found in our previous experiments with short echo time single voxel spectroscopy and phase encoded spectroscopic imaging (10). We detected singlet resonances from choline, creatine, and NAA, as well as multiplet resonances from compounds such as inositol, glutamine, and glutamate (Fig. 8). The SNR in spectra obtained at different depths was measured in selected data sets covering a wide range of acquisition times and voxel sizes. The normalized SNR at a given distance from the coil per square root of unit acquisition time and per unit volume (NSNR(x)) can be used to compare the SNR obtained with different parameter settings. For example, at a depth of 2–3 cm from the surface of the head, immediately adjacent to the region of outer volume suppression, the NSNR of the NAA resonance was between $0.5 \text{ s}^{-0.5} \text{ cm}^{-3}$ and $0.75 \text{ s}^{-0.5} \text{ cm}^{-3}$, a result consistent with our previous experience using surface coil single voxel spectroscopy. At a depth of approximately 6 cm from the surface of the head, the SNR of NAA decreased by approximately 50%, which is consistent with the expected sensitivity profile of the surface coil. The useful depth range measured from the edge of the lipid suppressed region was typically between 3 and 4 cm.

Lipid suppression pulses were tuned individually by observing the residual lipid signals from individual outer volume suppression slices (see Methods). The slice selection gradients for outer volume suppression were maximized within the constraints of the required slice width and the maximum RF power, to reduce chemical shift artifacts. Tuning parameters obtained in initial measurements were used for later measurements without further modifications. Residual lipid signals in the resulting EPSI data sets were less than or equal to the level of the metabolite resonances, except in some cases where errors in the positioning of the outer volume suppression were made.

DISCUSSION

EPSI provides an SNR per unit time and unit volume that is comparable with that obtained with conventional techniques at the same bandwidth per data point. Local gradients interfere with the echo formation in k -space and lead to aliasing artifacts which degrade the SNR unless even/odd echo editing is used. Proper phasing of each edited and processed data set is required to maintain the SNR in absorption mode spectra after adding the two

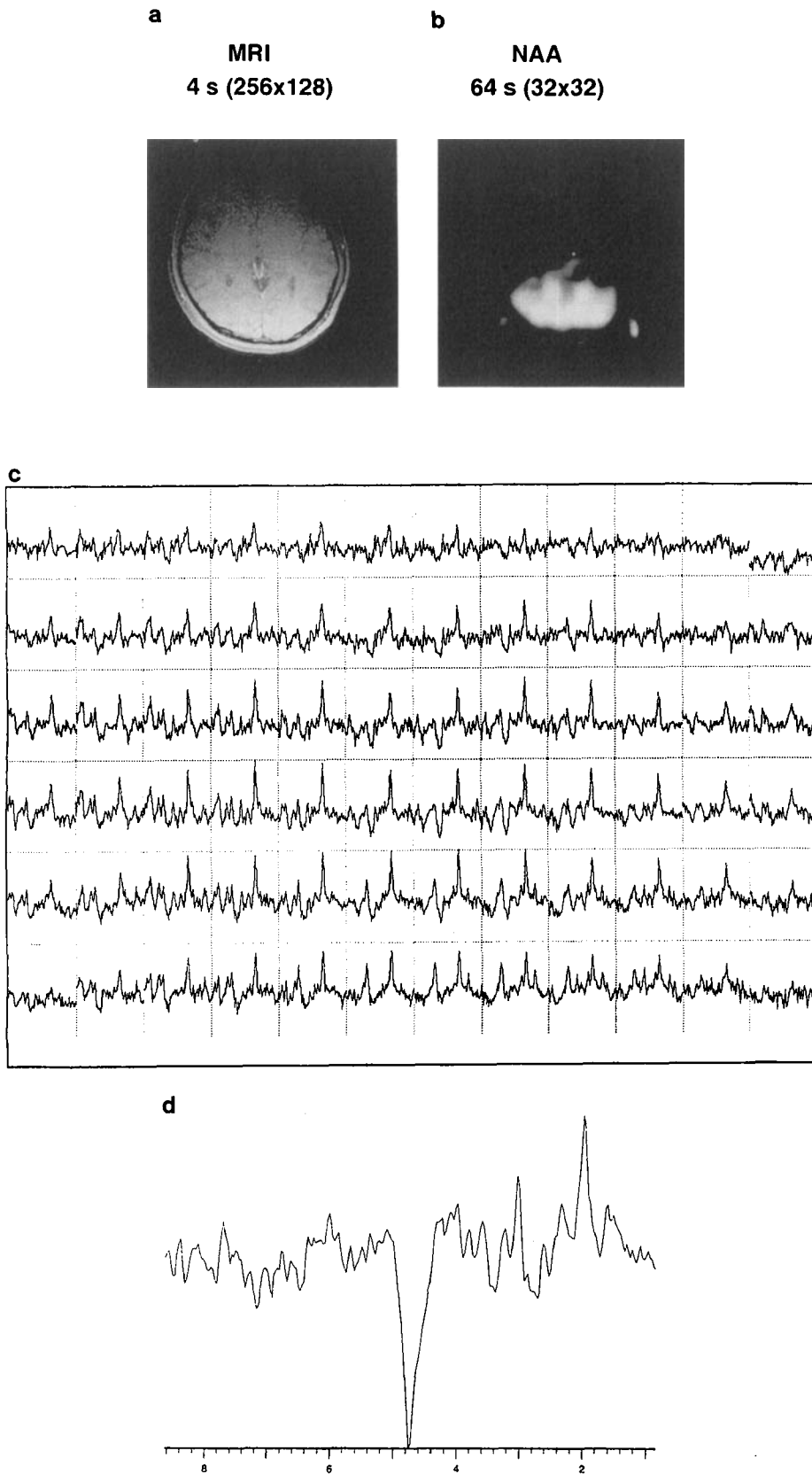


FIG. 7. EPI data set obtained on a normal volunteer in occipital brain in 1 min with a voxel size of 1.1 cc ($7.5 \times 7.5 \times 20 \text{ mm}^3$). (a) Gradient recalled echo localizer scan. (b) NAA map. (c) Zoomed spectral array from a subset of spectra in the proximity of the surface coil displaying a spectral range from 1.5 to 3.8 ppm. (d) Individual spectrum displaying the entire spectral range.

data sets. Because automatic phasing may fail due to residual water signals, we are currently exploring the possibility of using a nonwater-suppressed data set as a spectral reference for phasing. The extra acquisition time

for such a reference data set is short due to the speed of this encoding scheme.

The spatial resolution and spectral bandwidth are limited by gradient rise times and eddy current performance.

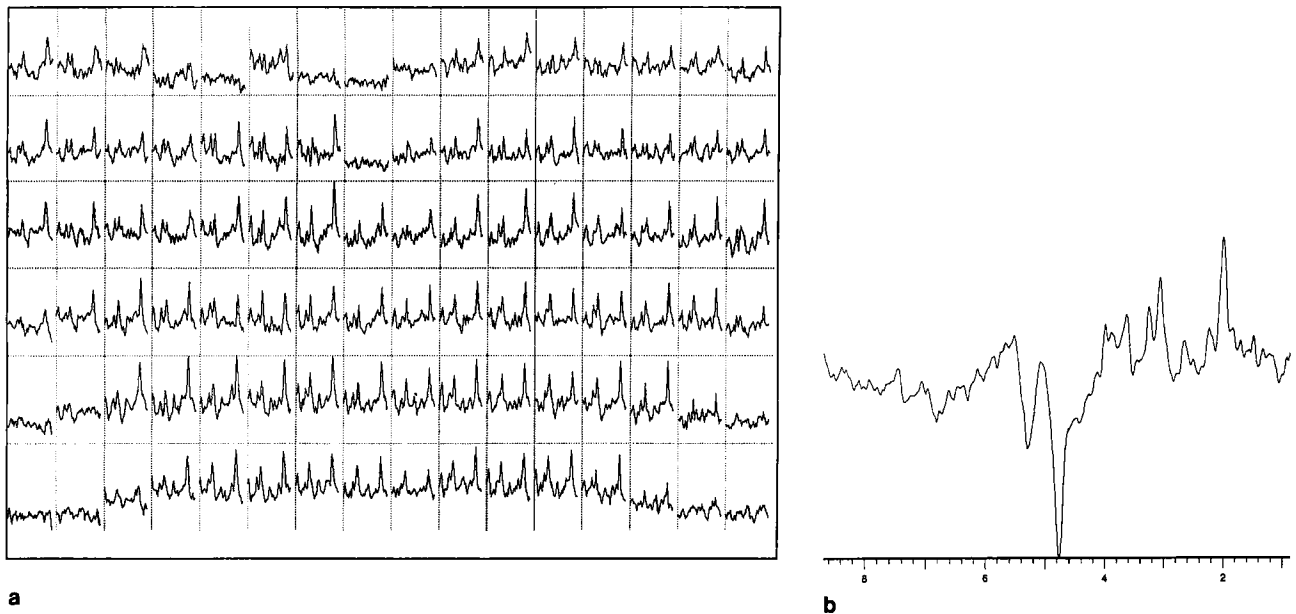


FIG. 8. EPSI data set obtained on a different normal volunteer from a similar anatomical location as in Fig. 7 with 16 averages (16 min acquisition time) and with a voxel size of 0.39 cc ($6.25 \times 6.25 \times 10 \text{ mm}^3$). (a) Zoomed spectral array from a subset of spectra in the proximity of the surface coil displaying a spectral range between 1.8 and 3.7 ppm. Localized signal losses in the top rows correspond to the ventricles. (b) Individual spectrum displaying the entire spectral range.

For HSI in human brain the SNR dictates voxel dimensions of at least 5 mm, which is the performance limit of our actively shielded gradients. Faster and stronger gradient systems that are increasingly available for whole body scanners will help to achieve a higher spatial resolution and a larger spectral bandwidth. The spatial-spectral localization scheme appears to be robust with small changes in gradient tuning and local magnetic field inhomogeneities as verified by application of shim gradients and detuning of the dephasing gradient. In these experiments the spectral resolution with EPSI is only limited by T_2^* -dephasing within the encoded voxels. With the application of EPSI read-out gradients, local gradients are rephased within the constraints of the encoded k -space similar to conventional phase encoding.

EPSI is quite similar to conventional fourier imaging with respect to encoding times and motion sensitivity. One constraint as compared with conventional imaging is the length of the data acquisition window, which limits multislice acquisitions to only a few slices per TR interval. If several averages are needed to obtain an adequate SNR, phase encoding in the third dimension becomes a useful alternative. Its advantages include the partial refocusing of local gradients, a continuous volume coverage and thin slice capabilities (24).

EPSI's short encoding time enhances the flexibility of spectroscopic imaging and permits shorter acquisition times when the SNR is adequate: With surface coils and surface coil phased arrays (28), the improved SNR in cortical brain permits reducing total acquisition times, which will improve the clinical acceptance of spectroscopic imaging. Faster spatial encoding will also help to more efficiently utilize the enhanced sensitivity at higher magnetic field strengths, which become increasingly available for human studies. Independent of SNR consid-

erations, EPSI also reduces the risk of motion artifacts that limit the use of spectroscopic imaging in some clinical conditions, for example, with children, cognitively impaired patients, and patients with movement disorders. It also enables multiple measurements under different experimental conditions and time courses. The flexibility of positioning and shaping the region of lipid suppression, as well as the degree of lipid suppression achieved with surface coils, enhance our capacity to study cortical brain structures close to lipid containing regions at short echo times.

ACKNOWLEDGMENTS

The authors thank Dr. Daniel Spielman for providing the software for automatic higher order shimming, Dr. Jeffrey R. Alger for stimulating discussions and encouragement during this work, Dr. Alessandro Bertolino for help with data analysis, and Dr. Geoffrey Sobering and GE Medical Systems for software support.

REFERENCES

1. P. R. Luyten, A. J. H. Marien, W. Heindel, P. H. J. van Gerven, K. Herholz, J. A. den Hollander, G. Friedmann, W. S. Heiss, Metabolic imaging of patients with intracranial tumors: ^1H MR spectroscopic imaging and PET. *Radiology* **176**, 791–799 (1990).
2. P. R. Luyten, P. C. van Ryen, L. C. Meinert, A. J. H. Marien, J. A. den Hollander, Identifying epilepsy, in "Proc., SMRM, 10th Annual Meeting, Amsterdam, 1990," p. 1009.
3. D. Spielman, J. Pauly, A. Macowski, D. Enzman, Spectroscopic imaging with multidimensional pulses for excitation: SIMPLE. *Magn. Reson. Med.* **19**, 67–84 (1991).
4. D. J. Meyerhoff, J. H. Duyn, L. Bachman, G. Fein, M. W. Weiner, Alterations of brain proton metabolites in HIV infection: Preliminary ^1H SI findings, in "Proc., SMRM, 11th

- Annual Meeting, San Francisco, 1991," p. 404.
5. D. L. Arnold, P. M. Matthews, G. F. Francis, J. O'Connor, J. P. Antel, Proton magnetic resonance spectroscopic imaging for metabolic characterization of demyelinating plaque. *Ann. Neurol.* **31**, 235–241 (1992).
 6. K. Herholtz, W. Heindel, P. R. Luyten, J. A. den Hollander, U. Pietrzyk, J. Voges, H. Kugel, G. Friedmann, W. D. Heiss, In-vivo imaging of glucose consumption and lactate concentration in human gliomas. *Ann. Neurol.* **31**, 319–327 (1992).
 7. J. H. Duyn, G. B. Matson, A. A. Maudsley, J. W. Hugg, M. W. Weiner, Human brain infarction: proton MR spectroscopy. *Radiology* **183**, 711–718 (1992).
 8. M. J. Fulham, A. Bizzi, M. Dietz, H-L. Shih, R. Raman, G. S. Sobering, J. A. Frank, A. J. Dwyer, J. R. Alger, G. DiChiro, Mapping of brain tumor metabolites with proton MR spectroscopic imaging: Clinical relevance. *Radiology* **185**, 675–686 (1992).
 9. C. T. W. Moonen, G. Sobering, P. C. M. van Zijl, J. Gillen, M. von Kienlin, A. Bizzi, Proton spectroscopic imaging of human brain. *J. Magn. Reson.* **98**, 556–575 (1992).
 10. S. Posse, B. Schuknecht, M. E. Smith, P. C. M. van Zijl, N. Herschkowitz, C. T. W. Moonen, Short echo time proton MR spectroscopic imaging. *J. Comput. Assist. Tomogr.* **17**, 1–14 (1993).
 11. J. H. Duyn, J. Gillen, G. Sobering, P. C. M. van Zijl, C. T. W. Moonen, Multisection proton MR spectroscopic imaging of the brain. *Radiology* **188**, 277–282 (1993).
 12. J. H. Duyn, C. T. W. Moonen, Fast proton spectroscopic imaging of human brain using multiple echoes. *Magn. Reson. Med.* **30**, 409–414 (1993).
 13. A. Haase, D. Matthaei, Spectroscopic FLASH imaging (SPLASH imaging). *J. Magn. Reson.* **71**, 550–553 (1987).
 14. D. B. Twieg, Multiple-output chemical shift imaging (MOCISI): A practical technique for rapid spectroscopic imaging. *Magn. Reson. Med.* **12**, 64–73 (1989).
 15. D. Norris, W. Dreher, Fast proton spectroscopic imaging using the sliced k -space method. *Magn. Reson. Med.* **30**, 641–644 (1993).
 16. A. R. Guimaraes, J. R. Baker, R. M. Weisskopf, B. R. Rosen, R. G. Gonzales, Echo planar metabolic imaging of brain, in "Proc., SMRM, 11th Annual Meeting, New York, 1993," p. 43.
 17. P. Mansfield, Spatial mapping of chemical shift in NMR. *Magn. Reson. Med.* **1**, 370–386 (1984).
 18. D. N. Guilfoyle, P. Mansfield, Chemical shift imaging. *Magn. Reson. Med.* **2**, 479–489 (1985).
 19. S. Matsui, K. Sekihara, H. Kohno, High-speed spatially resolved high-resolution NMR spectroscopy. *J. Am. Chem. Soc.* **107**, 2817–2818 (1985).
 20. S. Matsui, K. Sekihara, H. Kohno, High-speed spatially resolved NMR spectroscopy using phase-modulated spin-echo trains. Expansion of the spectral bandwidth by combined use of delayed spin-echo trains. *J. Magn. Reson.* **64**, 167–171 (1985).
 21. M. Doyle, P. Mansfield, Chemical shift imaging: a hybrid approach. *Magn. Reson. Med.* **5**, 255–261 (1987).
 22. S. Matsui, K. Sekihara, H. Kohno, Spatially resolved NMR spectroscopy using phase-modulated spin-echo trains. *J. Magn. Reson.* **67**, 476–490 (1986).
 23. P. Webb, D. Spielman, A. Macowski, A fast spectroscopic imaging method using a blipped phase encode gradient. *Magn. Reson. Med.* **12**, 306–315 (1989).
 24. S. Posse, C. DeCarli, D. LeBihan, 3D Echo-Planar MR spectroscopic imaging at short echo times in human brain. *Radiology*, **192**, 733–738 (1994).
 25. R. J. Ogg, P. B. Kingsley, J. S. Taylor, WET: A T_1 - B_1 -insensitive water suppression method for in vivo localized ^1H NMR spectroscopy. *J. Magn. Reson. Series B*, **104**(1), 1–10 (1994).
 26. A. H. Wilman, P. S. Allen, An analytical and experimental evaluation of STEAM versus PRESS for the observation of the lactate doublet. *J. Magn. Reson. Series B* **101**, 102–105 (1993).
 27. P. Webb, A. Macowski, Rapid, fully automatic, arbitrary-volume in vivo shimming. *Magn. Reson. Med.* **20**, 113–122 (1991).
 28. C. E. Hayes, J. S. Tsuruda, C. M. Mathis, Temporal lobes: surface MR coil phased array imaging. *Radiology* **189**, 918–920 (1993).